

We are IntechOpen, the world's leading publisher of Open Access books Built by scientists, for scientists

6,300

Open access books available

171,000

International authors and editors

190M

Downloads

Our authors are among the

154

Countries delivered to

TOP 1%

most cited scientists

12.2%

Contributors from top 500 universities



WEB OF SCIENCE™

Selection of our books indexed in the Book Citation Index
in Web of Science™ Core Collection (BKCI)

Interested in publishing with us?
Contact book.department@intechopen.com

Numbers displayed above are based on latest data collected.
For more information visit www.intechopen.com



Chapter

Metrology and Digital Image Processing in Dentistry

*Francisco Javier Cuevas de la Rosa, Miriam Rocha Navarro,
Manuel Garcia Salido and Manuel Rodríguez Villegas*

Abstract

Metrological techniques using digital image processing techniques have been extended into different fields of science such as optics, meteorology, mineralogy, agriculture, and medicine, among others. In the field of medicine, particularly in dentistry, it is important to perform different dental measurements to support the biometric work of specialists using panoramic radiographic images. Due to the poor capturing of these radiographic images, several problems, such as poor contrast and quality, are generally present. As the detection of the dental area must be done using these images, this chapter presents an algorithm that will assist in bettering image quality and make the dental measurements needed. This is done by binarizing using the histogram statistics of the image for the determination of threshold in order to establish sections of the teeth and the detection of the intramaxillary section by fitting a nonlinear function. The proposed method is applied to panoramic digital radiographs of subjects with permanent dentition (≥ 12 years and < 30 years). The algorithm achieved an adjustment of 96% of the processed radiographs as a result from patients of the School of Dentistry of the Universidad de la Salle Bajío.

Keywords: medical imaging, segmentation, panoramic X-ray images, biometrics, digital image processing, dental X-ray segmentation, polynomial regression, image thresholding

1. Introduction

Medical specialists in dentistry often use image analysis, most commonly using radiographs, to assist in making diagnoses and as support for planning out major and minor surgeries for a patient's treatment [1–14]. For this task, dentists and other specialists have relied on computational algorithms of Digital Image Processing and Optical Metrology to carry out the recognition of benign and malignant structures in bone tissue, delimit organs, and determine biometric characteristics that can be used in forensic tasks [15–18]. Unfortunately, due to problems in capturing radiographic images, such as noise, quality of film, inadequate adjustments of X-ray equipment parameters, and inexperience of radiological technicians, it is possible that medical specialist may incur errors during diagnosis.

Every day, dental pathologies in patients continue to increase, while the number of dentists worldwide is increasingly inadequate for the number of patients who require treatment in such a way that the development of automatic techniques for biometrics and dental metrology using Digital Image Processing and Artificial Intelligence is becoming of great importance. These techniques that carry out dental measurements are very useful to specialists because they assist in making diagnoses quicker and the follow-up after treatment easier [19–38]. Some of the most common ailments are periodontal disease, cavities, bone loss, chronic periapical abscess, periapical granuloma, radicular cyst, and malignant or benign tumors. Several of these conditions are monitored through dental biometric analysis using different X-ray images taken from different perspectives. The different perspectives used most frequently by dentists are periapical, bitewing and panoramic, or orthopantomograms. The panoramic perspective shows all the patient's teeth in one image making it possible to perform different measurements. Within the biometric process that must be done, there is the automatic detection and division of the intradental region and jaw (denture), since it is the starting point for performing dental segmentation and the detection of diastemas (intradental spacing).

It is also important to mention that there are other types of biometric applications using panoramic dental images where these algorithms can be applied. One alternative is using these dental images to identify people instead of using traditional methods such as face, iris, or fingerprint recognition in a forensic setting. Most often than not, the traditional methods mentioned can be damaged in serious incidents such as car and air accidents to the point where they cannot be used for biometric identification, so analysis and recognition from dental images is an excellent alternative for these forensic cases [15–18, 23].

Several researchers have worked on the development of manual and semiautomatic methods to detect and segment the jaw using different digital image processing algorithmic techniques. Several of the proposed methods require manual marking [15], which generates a disadvantage. Jain et al. [16, 17] proposed a method that uses an integral projection process of the image and Bayes rule to carry out the segmentation of the jaws and later an integration method for diastema detection. In [18], Wanat improved the method of Jain et al. by using splines to divide the jaws. The Jain and Chen algorithm [16] has continued to be improved and semiautomatic methods have been proposed; Harandi et al. [19] show a method for the segmentation of the intramaxillary region (IMR) through the use of modified geodesic active contour and different morphological operations on the X-ray image but it has some drawbacks due to the use of a cropped manually and that it works only with periapical images, in addition to the fact that the active detection of contours is an iterative process that can take up to 200 iterations. In [20], Hasan uses information from the gradient vector flow for the automatic adjustment of snakes in the image and the k-means method to perform the segmentation process. This method has the drawback that it is necessary to set the number of classes and the thresholding conditions manually. On the other hand, in [21], Haghanifar uses evolutionary computation and the Sauvola binarization algorithm to perform mandibular segmentation and separation; the jaw was divided using two steps: the calculation of the midpoints of the intradental zone and the use of snakes, which is computationally expensive. Recently, artificial intelligence and metaheuristic techniques have been used to carry out segmentation. In [22], Kong et al. propose a method that uses deep learning to carry out the detection of the maxillary region through an encoder and decoder network (EED-Net). This method has the

disadvantage that a marking and annotating process must be carried out by dental experts, which consumes the specialists' time and must be carried out manually, which complicates its application. Additionally, considerable time must be spent on training the EED-Net. On the other hand, in [23], an adjustment function is calculated with Particle Swarm Optimization as a metaheuristic process. This requires the manual selection of a series of points in the intramaxillary region, and a high-order polynomial is passed whose biggest problem is the oscillations it suffers due to this.

In this chapter, a method of segmentation using a polynomial function adjustment with coefficient estimation by the least squares approximation of the intramaxillary region (IMR) is proposed. The steps of the procedure are the following: (a) low-pass filter, (b) binarization using the gray-level frequency histogram, (c) calculation of centroids, (d) detection of the intramaxillary region (IMR), (e) detection of random points in the intramaxillary region, and (f) polynomial adjustment of parameters using least squares. The proposed method is applied to panoramic digital radiographs of subjects with permanent dentition (≥ 12 years and < 30 years). The following sections show the operation of each procedure of the proposed method, the experiments carried out, and the conclusions of the work.

2. Automatic intramaxillary region detection method

During the automatic biometric dental process, to give a diagnosis or treatment, it is essential to locate the intramaxillary region and detect the teeth of both jaws. To achieve this, an algorithm that performs the following steps is proposed: (a) smoothing by median filtering, (b) binarized with thresholding from the histogram, (c) detection of centroids, and (d) determination of the intramaxillary region. Each step of the proposed method is detailed below.

2.1 Image smoothed

Before starting with the IMR detection in the panoramic dental X-ray images, it is adequate to use spatial masks to perform spatial filtering processing. It is also possible to perform this same filtering but in the frequency domain by using the Fourier transform, although this is more laborious. In the case of panoramic dental X-ray images, it is prudent to carry out low-pass filtering that can reduce the noise effects related to high frequencies that are present in the Fourier domain because high-frequency components are related to the edges of objects, fine structures, and noise contained in images. Carrying out this process will result in an unfocused or blurred image due to the removal of this information by low-pass filtering. For these purposes, a Gaussian-type kernel or an averaging filter (statistical mean) can be used to remove high frequencies, but unfortunately in most cases they leave traces of noise and destroy important edges of the image. For this reason, for dental applications, it is preferred to work with the statistical method of the median since this method preserves the edges of the important dental pieces for segmentation tasks and dental biometry. In this method, the central pixel of the subimage mask around the (odd-sized) pixel is replaced by the statistical median instead of the value of the means or the application of the Gaussian spatial filter.

For IMR detection, it must be segmented into bright and dark regions. Given the *a priori* information of the images obtained from an X-ray process, the brightest regions of the image will be related to both compact and spongy bone tissue; on the other hand, the dark information is related to the other regions of the image among which is the IMR region of interest. It is important to eliminate high-frequency structures prior to the binarization process in order to improve its performance and avoid undesirable structures generated by spongy and compact bone tissue and additive noise contained in the image that prevent good IMR segmentation. To avoid this, a low-pass filter is applied beforehand using the statistical median of a neighborhood of pixels of size 11×11 . Using the set of values of the established neighborhood, we obtain the element that leaves half of the smaller elements below it and the other half above it, in such a way that the high-frequency elements in the region remain on the shores. This filter is applied because it better maintains the contours of the regions when binarizing, including the IMR zone of interest.

2.2 Thresholding

After having applied the filter to eliminate high frequencies of the X-ray image that interfere in the detection of the regions, the next step is to carry out the binarization process by thresholding to start the segmentation of dark regions where the IMR region is located. It is important and very common to use a thresholding method to be able to carry out a process of segmentation and partitioning of the image in binary form from the gray intensity levels of the image in this dental panoramic X-ray case. For this case, the global information of the X-ray image is used depending on the value of the pixel. The intent of these methods is to allow starting from the pixel value $I(x,y)$ at the spatial position of the digital dental panoramic X-ray image (x,y) , where each l -bit pixel can contain values in the range of $G \in [0, 2^l - 1]$ representing the gray levels of the image. The idea of thresholding procedures is to map each pixel from an original value $I: M \times N \rightarrow G$ to a function of only two possible values $B: M \times N \rightarrow \{0, 2^l - 1\}$ from a threshold value T such that the thresholding image can be represented as

$$B(x,y) = \begin{cases} 0, & \text{if } I(x,y) < T \\ 2^l - 1, & \text{if } I(x,y) \geq T \end{cases} \quad (1)$$

The intention is to find and design a robust criterion that can perform and be applied in a repeatable way the IMR segmentation to find an adequate threshold value T that can be used and ensure the detection of the region of interest depending on the value of each pixel in the original X-ray image $I(x,y)$. To carry out the segmentation for the initial detection of the IMR, the thresholding procedure is applied to the entire dental X-ray image with a single threshold value to generate the partition into dark and bright regions.

The IMR has the attributes of having a large area compared to the average of the regions in addition to having a centroid close to the center of the image because the dentist focuses the area of interest (teeth) in the capture process of the X-ray image. For this, we perform a binarization considering the *a priori* knowledge related to the fact that the concentration of bone tissue information is located in the bright section of the image and, therefore, recorded in the gray-level frequency histogram and that the remaining regions including the region of interest (IMR) are located in the region related to the frequency of dark gray levels.

Carrying out experimentation, a threshold was located that correctly segments the intradental region. To do this, we determine the probability distribution function of gray levels from the calculation of the histogram using the following expression:

$$p_i = \frac{h_i}{MN}, \quad (2)$$

where h_i is the frequency of occurrence of the gray level i , $M \times N$ is the resolution of the radiographic image, and p_i represents the probability of occurrence of the gray level; then, we determine the cumulative probability function using the following expression:

$$P_k = \sum_{i=0}^k p_i. \quad (3)$$

The optimal threshold detected by experimentation to determine the threshold T in the range of $[0,255]$, where the IMR is adequately separated, is when the cumulative probability function reaches 0.3, that is, the histogram represents 30% of the total resolution of the image; this can be expressed as

$$T \in \text{ArgMin} \left(\sum_{i=0}^T p_i > 0.3 \right) \quad (4)$$

$$T \in G \forall G = 0, 1, 2, \dots, 255.$$

From this threshold, the binarization of the image is carried out, from which several regions of different sizes related to the dark and bright information of the image are obtained. In the case of the IMR region of interest, it has the attribute of having an area with a larger dimension than the average of the other regions. To carry out the identification of this region, we eliminate the regions with a smaller area than the average of the total dark regions in order to speed up the detection process.

2.3 Calculation of centroids and IMR detection

After the binarized segmentation process of the dental X-ray images, it is important to determine some properties that can characterize them in order to discern the IMR region of interest in relation to the other partitions related to the dark regions of the X-ray image. One of the properties of the regions that are useful to carry out the IMR detection is undoubtedly the geometric information of the image and particularly its location of the centroids of the region. For this, it is necessary to calculate the areas of each region in the dark sections of the X-ray dental image and add the coordinates of these regions in rows and columns (x,y) so as to average the location of the pixels in the k region $R_k(x,y)$. From these images, the centroids (\bar{X}_k, \bar{Y}_k) of each region k ($R_k(\cdot)$) with area A_k are determined by calculating the following mathematical expressions:

$$\bar{X}_k = \frac{\sum_{x=0}^M \sum_{y=0}^N x R_k(x,y)}{A_k}, \bar{Y}_k = \frac{\sum_{x=0}^M \sum_{y=0}^N y R_k(x,y)}{A_k}. \quad (5)$$

Due to the fact that, when performing the capture, the dental specialist centers the patient's teeth on the X-ray plate, we can determine the IMR region from that region

whose centroid is closest to the center of the image in such a way that the IMR region will be the region k with the minimum indicated distance, that is,

$$k = \min_k \left(\sqrt{\left(\bar{X}_k - \frac{M}{2}\right)^2 + \left(\bar{Y}_k - \frac{M}{2}\right)^2} \right). \quad (6)$$

2.4 Polynomial fit to the intramaxillary region

Once the IMR intramaxillary region has been determined using the procedure outlined in the last process, the next step in the procedure consists of fitting a polynomial function expressed by

$$P_m(x) = a_0x^0 + a_1x^1 + a_2x^2 + \dots + a_mx^m, \quad (7)$$

that fits the patient's teeth from this region by fitting a smooth curve that minimizes the squared error Q of a sample of points from this region given by

$$Q = \sum_i^P [P_m(x_i) - y_i]^2. \quad (8)$$

For this, at least a sample of 2% of the points of the IMR region is used, that is, the number of points P will be greater than 0.2 of $M \times N$. Then, the following system of equations is solved to minimize the quadratic error related to the points of the region and the fit polynomial

$$\begin{bmatrix} n+1 & \sum x_i & \sum x_i^2 & \dots & \sum x_i^m \\ \sum x_i & \sum x_i^2 & \sum x_i^3 & \dots & \sum x_i^{m+1} \\ \vdots & \vdots & \vdots & \vdots & \vdots \\ \sum x_i^m & \sum x_i^{m+1} & \sum x_i^{m+2} & \dots & \sum x_i^{2m} \end{bmatrix} \begin{bmatrix} a_0 \\ a_1 \\ \vdots \\ a_m \end{bmatrix} = \begin{bmatrix} \sum y_i \\ \sum x_i y_i \\ \vdots \\ \sum x_i^m y_i \end{bmatrix}, \quad (9)$$

where (x_i, y_i) represent the sampled points of the IMR region and the vector $\mathbf{a} = (a_0, a_1, a_2, \dots, a_m)$ represents the coefficients of the fitted polynomial. A complete flowchart of the IMR region polynomial detection and fitting process is shown in **Figure 1**.

3. Experiments

This section shows examples of the segmentation process carried out on images of patients from the School of dentistry, Universidad La Salle, León, Mexico. The equipment with which the images were captured is Morita Veraview X800 X-ray equipment. The captured panoramic dental X-ray images have a resolution of 1935×1024 pixels. **Figure 2(a)** shows the panoramic image obtained by the X-ray equipment. To evaluate the performance of the method, the established process was carried out on 50 panoramic radiographic images of patients with age range between 12 and 30 years from the School of Dentistry, Universidad de La Salle Bajío, León, Guanajuato, Mexico, with the following inclusion and exclusion criteria:

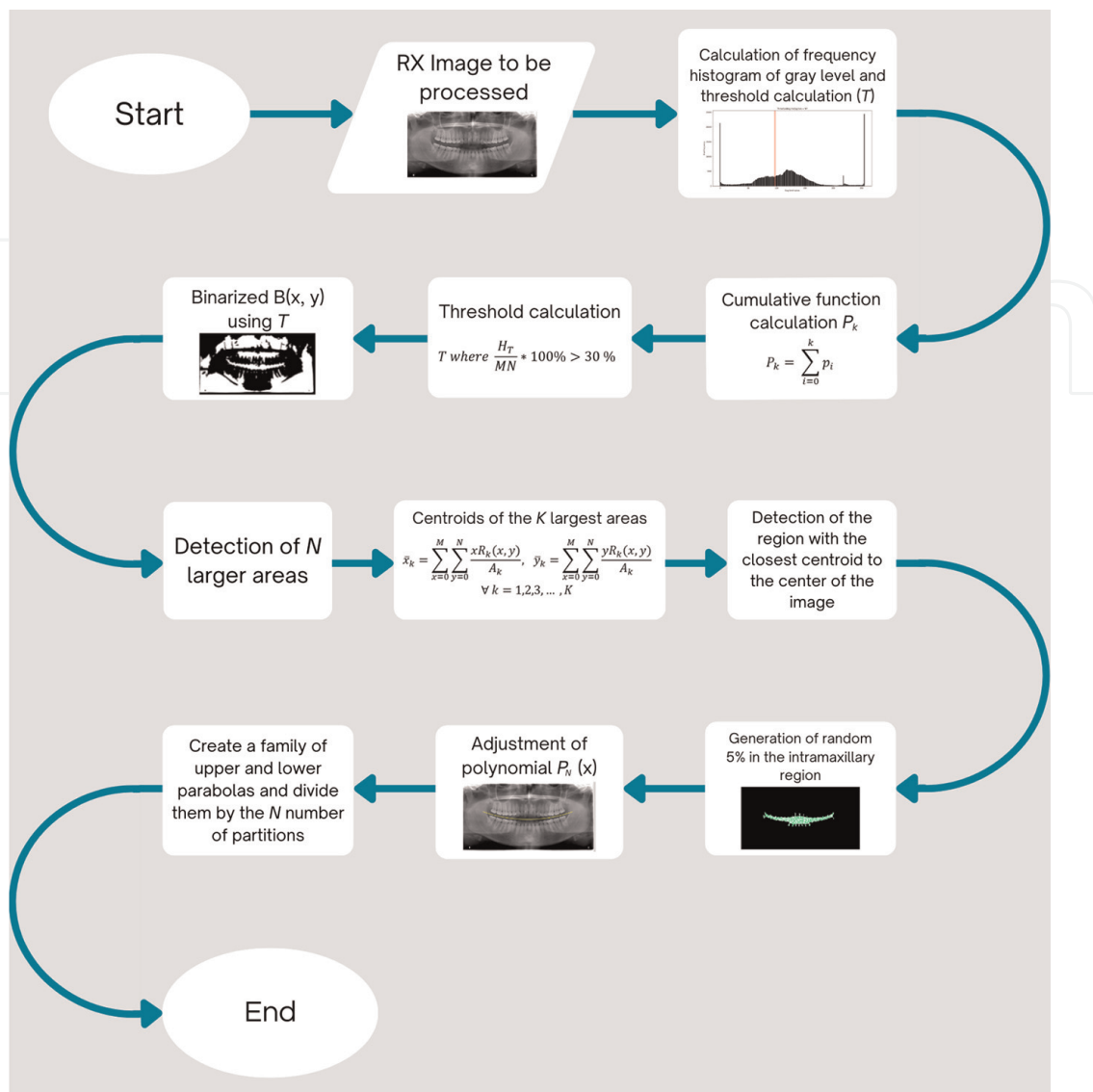


Figure 1.
 Flowchart of the IMR denture and jaw segmentation process.

a. *Inclusion Criteria*

- Panoramic digital radiographs of subjects with permanent dentition (≥ 12 years and < 30 years).
- Subjects of both genres.

b. *Exclusion criteria*

- Panoramic digital radiographs of subjects with teeth showing evidence of incisal or occlusal edge with restorative intervention, traumatic injury, or occlusal wear from bruxism.
- Radiographs showing mixed dentition or edentulism.

The first step in the procedure consists of filtering out high-frequency structures such as mandibular spongy and compact tissue and capture noise using a kernel that



Figure 2. (a) Original image. (b) Smoothed image using median filter size 11×11 where high-frequency structures (spongy and compact bone tissue) are removed.

calculates the median of a window of size 11×11 , the result of which is shown in **Figure 2(b)**.

After applying the low-pass filter (median), we calculated the gray-level frequency histogram of the panoramic dental image. From the generation of the histogram, we determine the probability distribution function using Eq. (2) and determine the value of the threshold T when the cumulative probability function reaches or exceeds 0.3. The histogram of the image of **Figure 1** and the detected threshold value (red line) is shown in **Figure 3**, and the binarized image with the threshold value T is shown in **Figure 4**.

The next step is to extract the centroids of the K largest regions and determine which of them is located closest to the center of the image, which is related to the IMR region of interest. **Figure 5** shows the largest areas from **Figure 4**, and **Figure 6** shows the related centroids. Finally, **Figure 7** shows the selected IMR region. Once the IMR region has been determined, the next step in the procedure necessary to carry out the

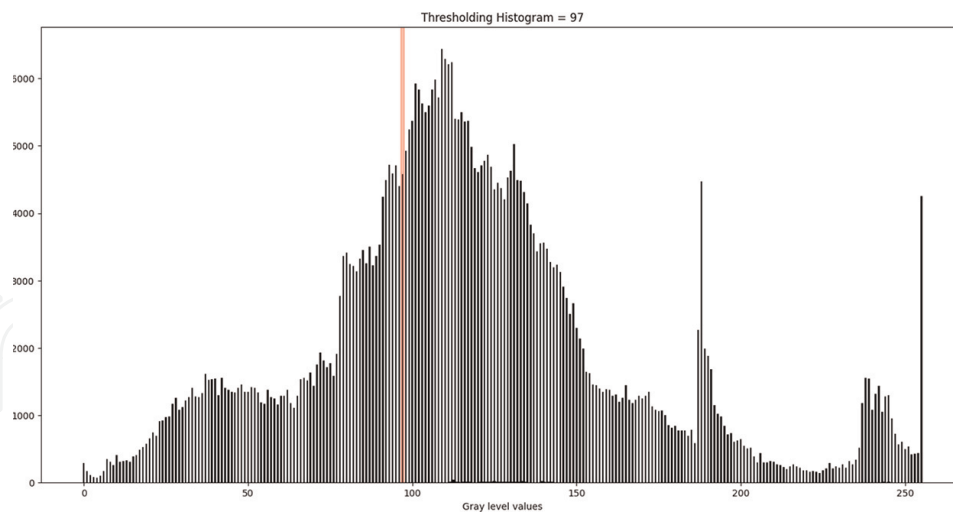


Figure 3.
Histogram with the frequency of occurrence of the gray levels of the image in Figure 1.



Figure 4.
Binarized image using a threshold of 30% from the cumulative function of the histogram of gray levels.



Figure 5.
Selection of the regions with the largest area from the binarized image in Figure 4.



Figure 6.
Centroids of the dark regions of the original image.



Figure 7.
Detection of the IMR region with centroid closest to the center of the image.

intramaxillary partition is to fit a polynomial (order 2) that smoothly divides the IMR. This is useful to carry out a subsequent process of dental biometric analysis. The fit is carried out by taking a sample of IMR points (2% of the points) and applying the optimization process to them to calculate the polynomial coefficients by estimating and reducing the mean square error by least squares. **Figure 8** shows the selected points and the fit of the curve (quadratic polynomial) that minimizes the error. **Figures 9** and **10** show the detection of the denture in both the lower and upper jaws on the original image. **Figure 11** shows eight additional results with images of different patients by using of the proposed method.

The efficiency of the method was calculated based on the total number of regions IMR divided correctly according to the established manual marking and qualified by dental specialists and the one that did not meet the established segmentation requirements. Then, the efficiency eq. E used for the proposed segmentation process was

$$E = \frac{C}{N} * 100\% \quad (10)$$

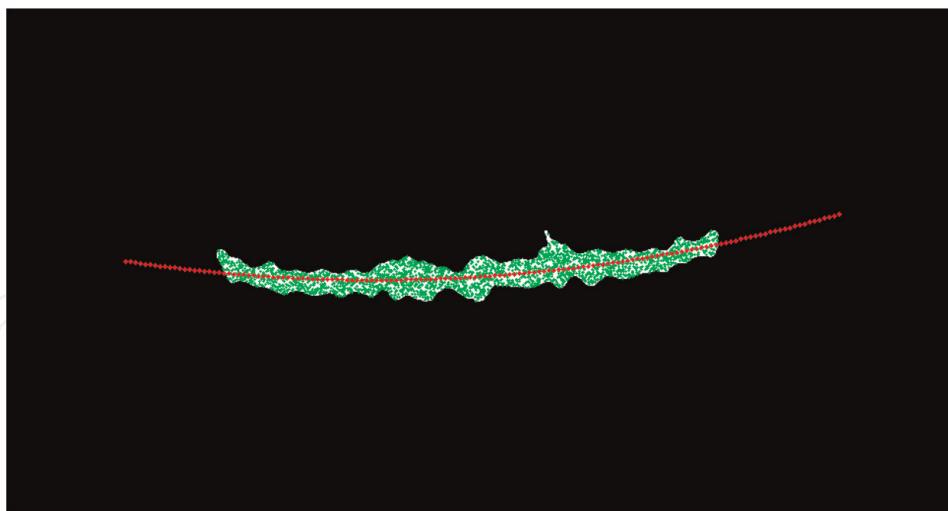


Figure 8.
Parabolic adjustment by point sampling in the binarized IMR region.

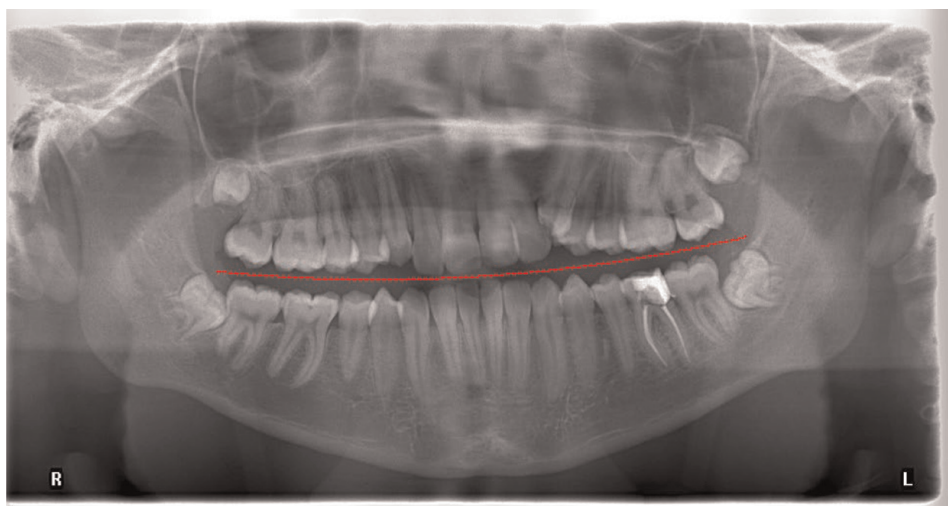


Figure 9.
Original image with a parabolic polynomial adjusted for division of the IMR section.

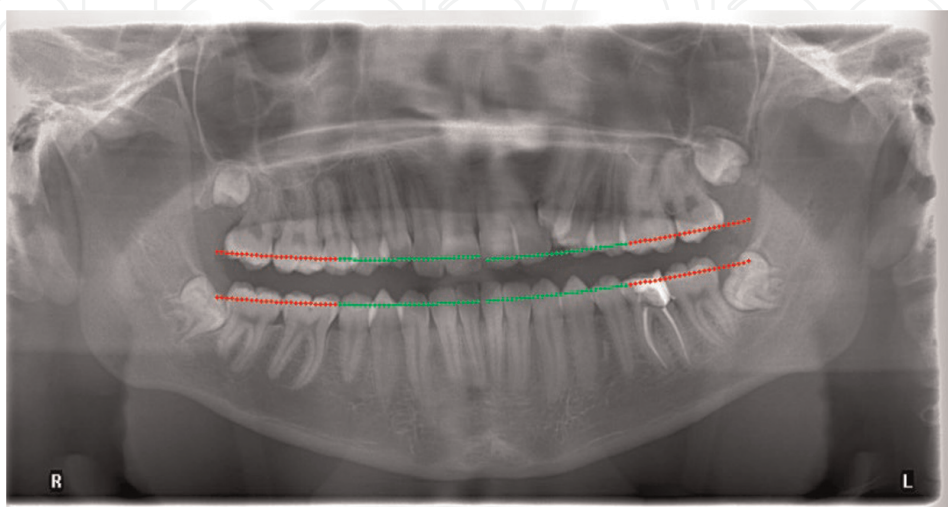
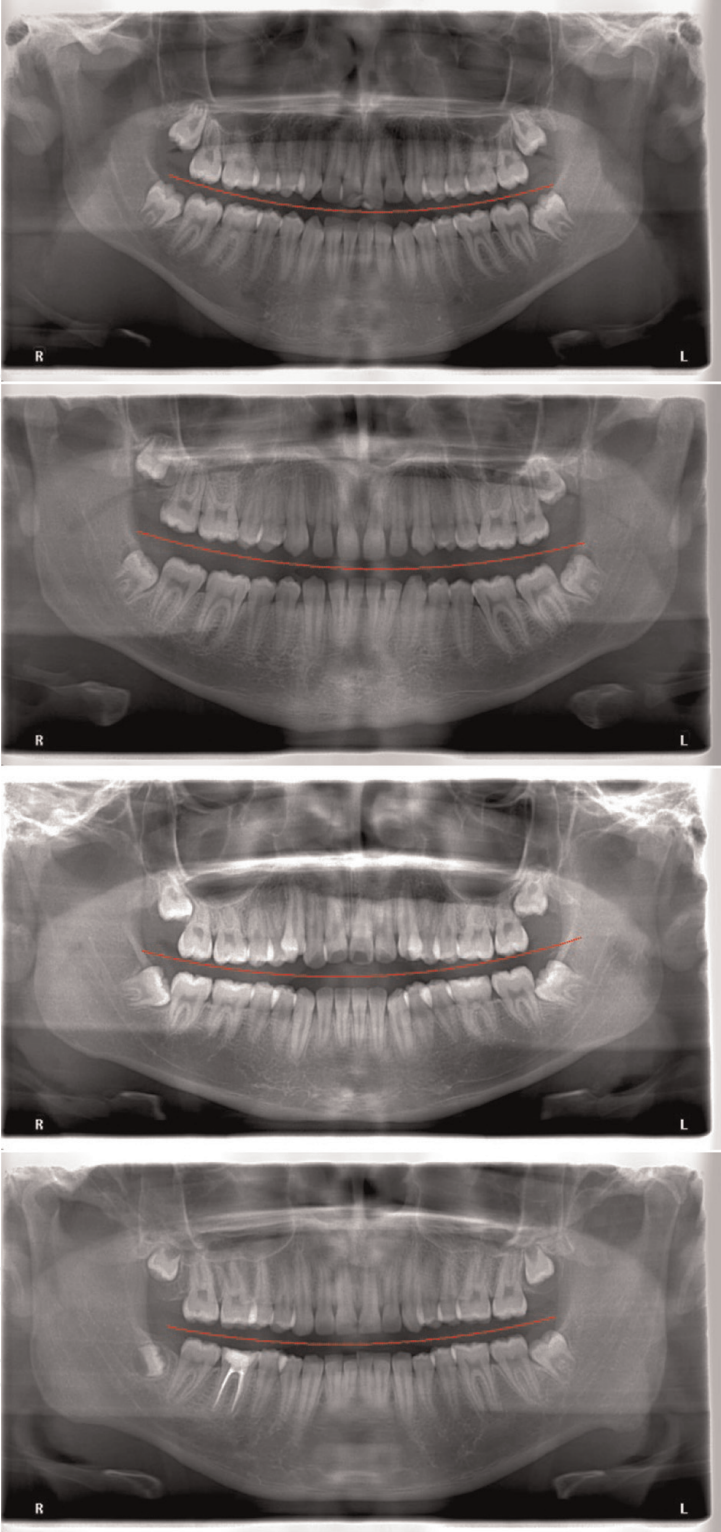


Figure 10.
Detection of the jaw in the lower and upper jaws.



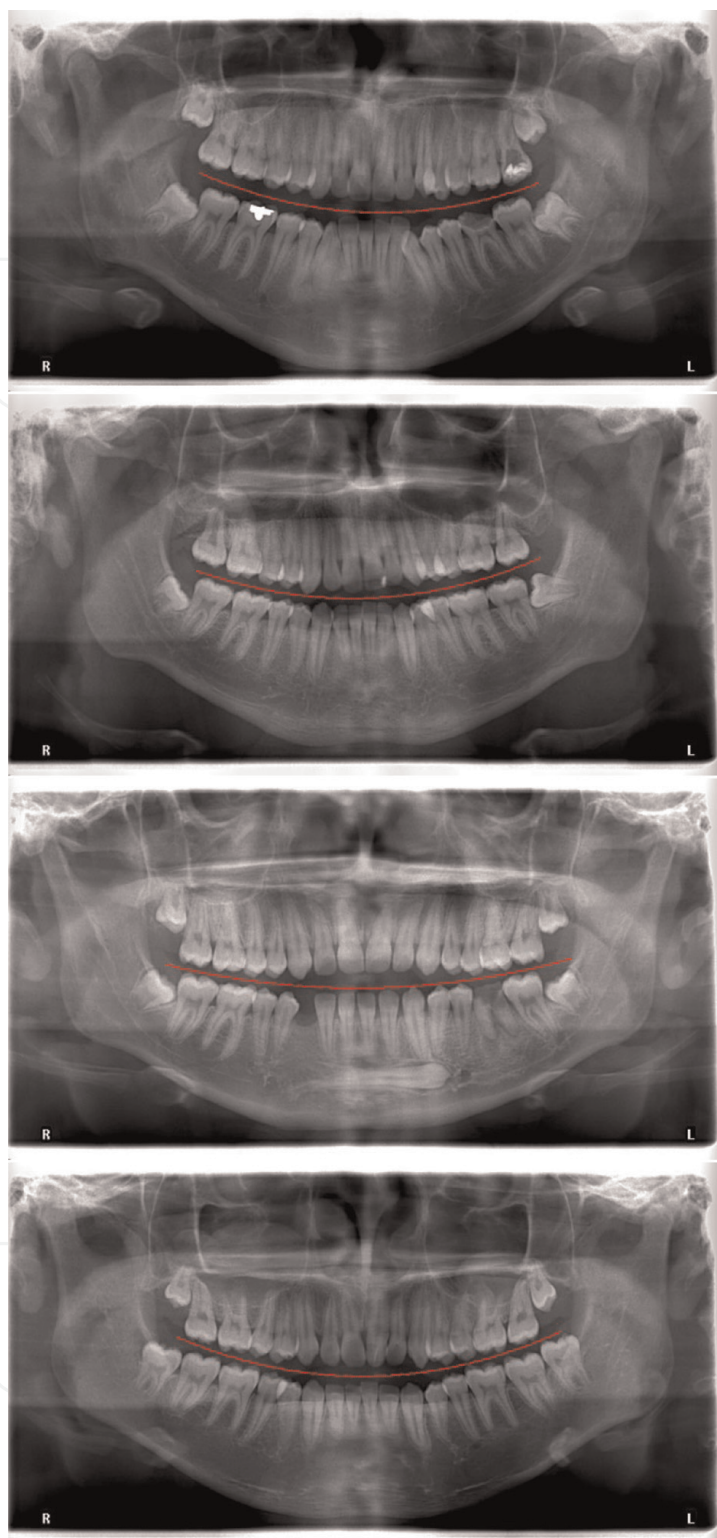


Figure 11.
Results using the proposed method applied to X-ray images from database with a curve fitting.

where C is the number of X-ray panoramic dental images well segmented according to dental specialists and N is the total number of processed X-ray panoramic dental images. Using the previous equation, the efficiency of the method to detect the mandible and IMR was calculated, which turned out to be 96%.

4. Conclusion

It is shown that it is possible to use the proposed method to carry out the division and recognition of the intramaxillary region automatically from panoramic X-ray images without requiring the assistance of a dental specialist. Among the improvements proposed in this chapter is the establishment of a thresholding method that adapts to the gray-level statistics of the dental X-ray image of the patient in order to determine the area of interest to be detected (IMR). The established method calculates the density and cumulative probability functions to determine the region of bone tissue and absent regions of this tissue where the IMR is located. Likewise, a function is proposed that minimizes the distance from the centroids of the dark regions related to the intramaxillary space, eliminating the bright regions related to the spongy and compact bone tissue for IMR detection. Then, a random sample of points from the IMR region is used to fit a quadratic polynomial that fits this region and the teeth. This procedure is carried out without requiring the assistance of a dental specialist. This detection method is useful for biometric measurements of teeth. The method was tested with 50 images and had an efficiency greater than 96%. Future work includes diastema detection and automatic segmentation of teeth for diagnostic and biometric tasks to monitor treatment and forensic applications, as well as a biometric dental support application for the daily work of dentists.

Acknowledgements

The authors wish to thank the Government of the state of Guanajuato in Mexico for supporting this research work under the fund IDEAGTO/CONV/079/2021-Ciencia Productiva- I + D Sociales y Humanidades en Sectores Estrategicos. The authors would like to thank the following people for their support: Martha Eugenia Fajardo Araujo, Juan Manuel Lopez, Fatima Hernandez Alvarez, Kenya Garcia Garcia, Hector Eduardo Gomez Perez, Alessio Sanchez Blasutti, and Karina Guerrero Abrego who were a fundamental part of the development of the work. The authors also thank the following institutions whose facilities and financial support were important in the development of the research: Centro de Investigaciones en Óptica, A.C, Universidad de la Salle Bajío and Instituto Tecnológico y de Estudios Superiores de Monterrey, CONACYT, and Universidad de Guanajuato.

IntechOpen

Author details

Francisco Javier Cuevas de la Rosa^{1*}, Miriam Rocha Navarro², Manuel Garcia Salido³
and Manuel Rodríguez Villegas⁴

1 Centro de Investigaciones en Óptica, A.C, México


2 Faculty of Dentistry, Universidad de la Salle Bajío, A.C, México

3 UNITEC Campus Leon, México

4 Universidad De La Salle Bajío, A.C, México

*Address all correspondence to: miriamrocha@yahoo.com

IntechOpen

© 2023 The Author(s). Licensee IntechOpen. This chapter is distributed under the terms of the Creative Commons Attribution License (<http://creativecommons.org/licenses/by/3.0>), which permits unrestricted use, distribution, and reproduction in any medium, provided the original work is properly cited. 

References

- [1] Iannucci JM, Howerton LJ. *Dental Radiography: Principles and Techniques*. 5th ed. St. Louis, MO: Elsevier/Saunders; 2017
- [2] Whaites E, Drage N. *Essentials of Dental Radiography and Radiology*. 5th ed. Edinburgh: Elsevier; 2013
- [3] Gonzalez RC, Woods RE. *Digital Image Processing*. 4th ed. Upper Saddle River, NJ: Pearson; 2017
- [4] Sonka M, Fitzpatrick JM, editors. *Handbook of Medical Imaging. Medical Image Processing and Analysis*. Vol.2. Bellingham: SPIE Press; 2000. DOI: 10.1117/3.831079
- [5] Risnes S, Segura JJ, Casado A, Jiménez-Rubio A. Enamel pearls and cervical enamel projections on 2 maxillary molars with localized periodontal disease: Case report and histologic study. *Oral Surgery, Oral Medicine, Oral Pathology, Oral Radiology, and Endodontology*. 2000; **89**(4):493-497. DOI: 10.1016/s1079-2104(00)70131-4
- [6] Hellén-Halme K, Nilsson M, Petersson A. Digital radiography in general dental practice: A field study. *Dentomaxillofacial Radiol*. 2007;**36**(5): 249-255. DOI: 10.1259/dmfr/95125494
- [7] Ennes J, Lara V. Comparative morphological analysis of the root developmental groove with the palato-gingival groove. *Oral Diseases*. 2004; **10**(6):378-382. DOI: 10.1111/j.1601-0825.2004.01009.x
- [8] Anjna E, Kaur ER. Review of image segmentation technique. *International Journal of Advanced Research in Computer Science*. 2017;**8**(4):36-39. DOI: 10.26483/IJARCS.V8I4.3691
- [9] Bansal GJ. Digital radiography. A comparison with modern conventional imaging. *Postgraduate Medical Journal*. 2006;**82**(969):425-428. DOI: 10.1136/pgmj.2005.038448
- [10] Fujita M, Kodera Y, Ogawa M, Wada T, Doi K. Digital image processing of periapical radiographs. *Oral Surgery, Oral Medicine, and Oral Pathology*. 1988;**65**(4):490-494. DOI: 10.1016/0030-4220(88)90365-9
- [11] Gormez O, Yilmaz HH. Image post-processing in dental practice. *European Journal of Dentistry*. 2009;**3**(4):343-347
- [12] Goldstein AR. Enamel pearls as contributing factor in periodontal breakdown. *The Journal of the American Dental Association*. 1979;**99**(2):210-211. DOI: 10.14219/jada.archive.1979.0258
- [13] Said E, Fahmy GF, Nassar D, Ammar H. Dental X-ray image segmentation. *Biometric Technology for Human Identification*. 2004;**25**:409-417. DOI: 10.1117/12.541658
- [14] Stolojescu-Crisan C, Holban S. A comparison of X-ray image segmentation techniques. *Advances in Electrical and Computer Engineering*. 2013;**13**(3):85-92. DOI: 10.4316/aece.2013.03014
- [15] Omanovic M, Orchard JJ. Image registration-based approach to ranking dental x-ray images for human forensic identification. *Canadian Society of Forensic Science Journal*. 2008;**41**(3): 125-134. DOI: 10.1080/00085030.2008.10757170
- [16] Jain AK, Chen H, Minut S. Dental biometrics: Human identification using dental radiographs. In: *Lecture Notes in*

Computer Science. Berlin Heidelberg: Springer-Verlag; 2003. pp. 429-437. DOI: 10.1007/3-540-44887-x_51

[17] Jain AK, Chen H. Matching of dental X-ray images for human identification. *Pattern Recognition*. 2004;**37**(7): 1519-1532. DOI: 10.1016/j.patcog.2003.12.016

[18] Wanat R. A problem of automatic segmentation of digital dental panoramic x-ray images for forensic human identification. In: *Proceedings of CESC: The 15th Central European Seminar on Computer Graphics*. Slovakia: Vinicné; 2011

[19] Harandi AA, Pourghassem H, Mahmoodian H. Upper and lower jaw segmentation in dental X-ray image using modified active contour. In: *2011 international conference on intelligent computation and biomedical instrumentation*. Wuhan, Hubei, China: IEEE; 2011

[20] Hasan MM, et al. Automatic segmentation of jaw from panoramic dental X-ray images using GVF snakes. In: *2016 World Automation Congress (WAC)*. Rio Grande, Puerto Rico: IEEE; 2016. DOI: 10.1109/wac.2016.7583022

[21] Haghanifar A, Majdabadi MM, Ko SB. Automated teeth extraction from dental panoramic x-ray images using genetic algorithm. In: *2020 IEEE International Symposium on Circuits and Systems (ISCAS)*. Sevilla, Spain: IEEE; 2020. DOI: 10.1109/iscas45731.2020.9180937

[22] Kong Z, Xiong F, Zhang C, et al. Automated maxillofacial segmentation in panoramic dental x-ray images using an efficient encoder-decoder network. *IEEE Access*. 2020;**8**:207822-207833. DOI: 10.1109/access.2020.3037677

[23] Bozkurt MH, Karagol S. Jaw and teeth segmentation on the panoramic x-ray images for dental human identification. *Journal of Digital Imaging*. 2020;**33**(6):1410-1427. DOI: 10.1007/s10278-020-00380-8

[24] Sezgin M, Sankur B. Survey over image thresholding techniques and quantitative performance evaluation. *Journal of Electronic Imaging*. 2004; **13**(1):146. DOI: 10.1117/1.1631315

[25] Gayathri V, Menon HP. Challenges in edge extraction of dental x-ray images using image processing algorithms – A review. *International Journal of Computer Science and Information Technologies*. 2014;**5**(4):5355-5357

[26] Amer YY, Aqel MJ. An efficient segmentation algorithm for panoramic dental images. *Procedia Computer Science*. 2015;**65**:718-725. DOI: 10.1016/j.procs.2015.09.016

[27] Pham DL, Xu C, Prince JL. Current methods in medical image segmentation. *Annual Review of Biomedical Engineering*. 2000;**2**(1):315-337. DOI: 10.1146/annurev.bioeng.2.1.315

[28] Liao P, Fan Y, Nathanson D. Evaluation of maxillary anterior teeth width: A systematic review. *The Journal of Prosthetic Dentistry*. 2019;**122**(3):275-281. e7. DOI: 10.1016/j.prosdent.2018.10.015

[29] McGowan S. Characteristics of teeth: A review of size, shape, composition, and appearance of maxillary anterior teeth. *Compendium of Continuing Education in Dentistry*. 2016;**37**(3):164-quiz172

[30] Tsukiyama T, Marcushamer E, Griffin TJ, Arguello E, Magne P, Gallucci GO. Comparison of the anatomic crown width/length ratios of unworn and worn maxillary teeth in

Asian and white subjects. *The Journal of Prosthetic Dentistry*. 2012;**107**(1):11-16. DOI: 10.1016/S0022-3913(12)60009-2

[31] Orozco-Varo A, Arroyo-Cruz G, Martínez-de-Fuentes R, Jiménez-Castellanos E. Biometric analysis of the clinical crown and the width/length ratio in the maxillary anterior region. *The Journal of Prosthetic Dentistry*. 2015; **113**(6):565-70.e2. DOI: 10.1016/j.prosdent.2014.11.006

[32] Al-Khatib AR, Rajion ZA, Masudi SM, Hassan R, Anderson PJ, Townsend GC. Tooth size and dental arch dimensions: A stereophotogrammetric study in southeast Asian Malays. *Orthodontics & Craniofacial Research*. 2011;**14**(4): 243-253. DOI: 10.1111/j.1601-6343.2011.01529.x

[33] Fernandes TM, Sathler R, Natalício GL, Henriques JF, Pinzan A. Comparison of mesiodistal tooth widths in Caucasian, African and Japanese individuals with Brazilian ancestry and normal occlusion. *Dental Press Journal of Orthodontics*. 2013;**18**(3):130-135. DOI: 10.1590/s2176-94512013000300021

[34] Reynoso Rodríguez JL. Segmentation of molars in noisy pantomograms using digital image processing techniques. In: Master in Optomechatronics [thesis]. León, Mexico: Centro de Investigaciones en Óptica; 2017

[35] Garcia-Alcala LM. Segmentation of X-Ray Dental Panoramic Images by Using of Digital Image Processing, Computer Sciences Engineering [Bachelor Thesis]. León, México: Instituto Tecnológico de Zamora; 2020

[36] Gomez HE. Algorithm for the Automatic Segmentation of Panoramic Dental X-Ray Images by Using of

Techniques of Digital Image Processing and Artificial Intelligence, Technical Report on Professional Residence of Computer Science Engineering at CIO. León, México: Instituto Tecnológico de Leon; 2021

[37] Hutter F, Kotthoff L, Vanschoren J. *Automated Machine Learning: Methods, Systems, Challenges*. 1st ed. Cham, Switzerland: Springer International Publishing; 2019

[38] Engelbrecht AP. *Computational intelligence: an introduction*. The Atrium, Southern Gate, Chichester, West Sussex, England: John Wiley & Sons Ltd; 2007